Assignments and Conformational Dependencies of the Amide III Peptide Backbone UV Resonance Raman Bands

Alexander V. Mikhonin, Zeeshan Ahmed, Anatoli Ianoul, and Sanford A. Asher*

Department of Chemistry, University of Pittsburgh, Pittsburgh, Pennsylvania 15260

Received: September 7, 2004

We investigated the assignments and the conformational dependencies of the UV resonance Raman bands of the 21-residue mainly alanine peptide (AP) and its isotopically substituted derivatives in both their α-helical and PPII states. We also examined smaller peptides to correlate conformation, hydrogen bonding, and structure. Our vibrational mode analysis confirms the complex nature of the amide III region, which contains many vibrational modes. We assign these bands by interpreting the isotopically induced frequency shifts and the conformational sensitivity of these bands and their temperature dependence. Our assignments of the amide bands in some cases agree, but in other cases challenge previous assignments by Lee and Krimm (*Biopolymers* **1998**, *46*, 283−317), Overman and Thomas (*Biochemistry* **1998**, *37*, 5654−5665), and Diem et al. (*J. Phys. Chem.* **1992**, *96*, 548−554). We see evidence for the partial dehydration of α-helices at elevated temperatures.

Introduction

UV resonance Raman spectroscopy[1] (UVRS) has recently been demonstrated to be a powerful tool for studying the early stages in protein folding.[2−4] The power of the methodology stems from its ability to easily utilize the numerous amide vibrational bands which occur within the 500−2000 cm^{-1} Raman frequency region to probe peptide and protein secondary structure. The amide backbone vibrational frequencies and their normal mode compositions depend sensitively on the peptide backbone secondary structure.[2,3,5−8] For example, the amide III (AmIII) vibrational mode composition depends sensitively on the peptide bond's Ramachandran dihedral angles.[7−9] This sensitivity of vibrational frequencies to conformation is the basis for the use of vibrational spectroscopy to study molecular structure in general.

The use of vibrational spectroscopy to study protein secondary structure has a long and distinguished history.[10−12] Recent advances in the theory and practice of vibrational spectroscopy indicate that vibrational spectroscopy will continue to evolve more incisive methods to determine peptide and protein structure.[13,14]

Infrared absorption studies generally are limited to examining proteins and peptides in D_2O[13,15,16] to avoid the overwhelming water absorption.[17] IR studies of proteins and peptides in D_2O allow the study of the AmI′ and AmII′ bands (where the slanted prime designates vibrations from amides which have exchanged their amide NH with deuterium); the AmI′ band frequency clearly depends on the protein secondary structure.[13,18−20] Vibrational circular dichroism (VCD) gives additional information on protein and peptide secondary structure.[21−26]

Raman measurements show little interference from water,[10] and thus, the Raman spectra display numerous amide bands including the AmI, AmII, and AmIII bands, as well as other backbone bands.[2,5,27−31] In normal Raman spectra excited in the near-IR or visible spectral region, these bands overlap side-chain bands,[29,32,33] and often, only the AmI band is well resolved, although the amide III bands can often also be observed. The AmII band is not observed in the absence of resonance excitation.[34] Raman optical activity (ROA) can give additional insight into the secondary structure because of its sensitivity to backbone conformation.[35−39]

Excitation in the UV region enhances numerous Raman bands of the backbone amide peptide bonds.[2,5,30,40−44] These bands include the AmI, AmII, and AmIII bands, as well as a mainly C_α−H bending vibration which mixes with the AmIII vibration to a degree which depends on the backbone Ramachandran dihedral angles.[7−9,43,45] This mixing leads to conformationally sensitive UV−Raman spectra that can be analyzed to obtain quantitative secondary structure information.[2,5]

The challenge in interpreting the peptide bond vibrational spectra is that there is an incomplete understanding of the amide vibrational modes, despite years of excellent experimental and theoretical studies. The spectral region encompassing the AmIII spectral region is the least understood; as a result, the normal-mode composition of the AmIII bands still remains under intense investigation. For example, Oboodi et al.'s Raman[46] and Diem et al.'s VCD[47,48] isotopic substitution studies identified at least three AmIII bands in alanylalanine and proposed that these bands originate from mixing among N−H in-plane, (N)C_α−H, and (C)C_α−H bending (b) vibrations. Lee and Krimm's[49−51] theoretical and experimental studies of α-helical poly(alanine) also revealed significant complexity in the AmIII region. Their normal-mode analysis proposed contributions of C−N stretch (s), N−H in-plane bending (ib), C_α−H b, and C_α−C s modes to the observed AmIII region bands. More recently, Overman and Thomas's Raman isotopic substitution studies of α-helical filamentous virus demonstrated difficult-to-reconcile features in the AmIII and C_α−H bending spectral region.[27,33,52] Although they proposed that all of their viral protein classical AmIII bands involving C−N s and N−H b occur only below ∼1310 cm^{-1}, they demonstrated that the largest C_α−D substitution isotopic frequency dependencies occurred at ∼1345 cm^{-1}!

In our study here, we reexamine the UV−Raman enhanced amide vibrational bands of the peptide backbone, especially the amide III vibrations. We should note that our interpretations of the vibrational spectra are aided by the fact that the amide bonds

* Phone: 412-624-8570. Fax: 412-624-0588. E-mail: asher@pitt.edu.

10.1021/jp045959d CCC: $27.50 © 2004 American Chemical Society
Published on Web 11/18/2004

independently Raman scatter, and there is little complication of the spectra by the coupling of vibrational motion between amides.[53,54]

In this study, we examine the AmIII region of a 21-residue, mainly Ala, peptide (AP) and smaller peptides. The AP peptide is an excellent model, because we have shown that, at temperatures below room temperature, the AP Raman spectra can be described as the sum of the spectra of α-helical and polyproline II (PPII) conformations.[2,9] At temperatures above room temperature, AP is predominantly PPII.[2,9] Time-resolved Raman studies of AP revealed that fast monoexponential α-helix melting occurs with a relaxation time of about 200 ns.[2,3] Melting from the α-helix to the PPII state spectrally appears to be a two-state process without any evidence of significantly populated intermediate states.[2,3,9] We originally thought that the AP unfolded state was a disordered random coil state.[2,3] However, we recently demonstrated that it is predominantly a PPII helix.[9]

In this work, we examine the assignments of UVRS backbone amide bands of AP in both its α-helical and PPII states by using isotopic substitutions that dramatically change the amide group normal-mode composition, by using resonance Raman enhancement of these bands, and by using the temperature dependence of the amide band frequencies of each conformational state, which gives information on the contribution of N—H bending, C—N stretching, and C═O stretching to these vibrations.

Experimental Section

Sample Preparation. The 21-residue alanine-based peptide $AAAAA(AAARA)_3A$ (AP) was prepared (HPLC pure) at the Pittsburgh Peptide Facility by using the solid-state peptide synthesis method. All AP samples contained 1 mg/mL AP and included 0.2 M sodium perchlorate as an internal standard.

The 21-residue alanine-based AdP peptide of sequence **AAAAAAAA**RAAAAR**AAAAR**AA (where **A** is L-alanine (2,3,3,3-D_4), R is L-arginine, and A is normal-abundance L-alanine) was prepared (HPLC pure) at the Pittsburgh Peptide Facility and at Anaspec Corp. (San Jose, CA) using the solid-state peptide synthesis method. AdP is a perdeuterated AP peptide, except for the R residues and the central A_{10}—A_{13} residues; essentially all but the internal 6 residues R_9AAAAR_{14} are perdeuterated (except R_{19}). All AdP samples contained 0.5 mg/mL AdP and included 0.15 M sodium perchlorate. All Raman spectra were normalized to the intensity of the 932-cm^{-1} ClO_4^- Raman band. Prior to the UVRS measurements, the AP and AdP in D_2O solutions were kept at +62 °C for 5 min to ensure complete N-deuteration.

Short poly(alanine) peptides A_n (n = 2, 3, ..., 6) as well as Ala-Asp and Val-Lys dipeptides were purchased from Bachem Bioscience Inc. (King of Prussia, PA) and used as received in water solutions. We utilized peptide concentrations in water between 0.15 and 5 mg/mL. Sodium perchlorate (0.1—0.15 M) was used in each solution as an internal standard.

Ala-Asp, Val-Lys, and Ala-Ala crystals were prepared by growing them directly from water solution. All crystal structures and Ψ and Φ dihedral angles were obtained from X-ray diffraction measurements at the University of Pittsburgh and/or from literature X-ray diffraction studies. *N*-methylacetamide (NMA, Aldrich) concentrations in both water and D_2O were ~0.033 M (5 mL of NMA in 20 mL of water/D_2O).

Instrumentation. The UV resonance Raman instrumentation has been described in detail elsewhere.[2,3] A Coherent Infinity Nd:YAG laser produced 355-nm (third harmonic) 3-ns pulses at 100 Hz. This beam was Raman-shifted to 204 nm (fifth anti-Stokes) by using a 1-m tube filled with hydrogen (60 psi). A Pellin Broca prism was used to select the 204-nm excitation beam. The Raman scattered light was imaged into a subtractive double spectrograph and the UV light was detected by either a Princeton Instruments solar blind intensified charge-coupled device (ICCD) camera or a Roper Scientific unintensified liquid-nitrogen-cooled CCD camera. All samples were measured in a thermostatted free-surface flow stream.

UVRS powder crystal spectra, as well as some solution spectra of short peptides, were measured by using the 229-nm line of a continuous wave (CW) doubled Ar^+ laser. The scattered light was collected by a Spex Triplemate spectrograph coupled to a Princeton Instruments solar blind ICCD camera.

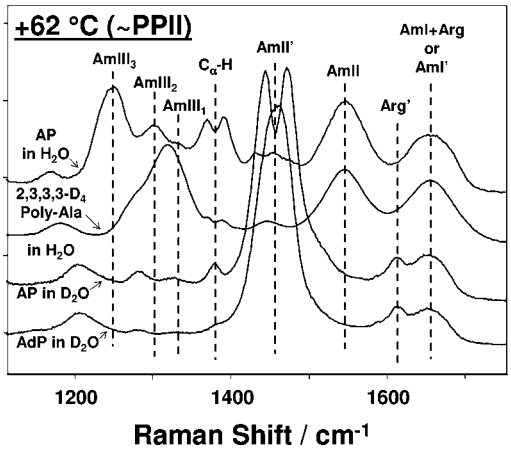

Figure 1. (a) 204-nm UVRS at 62 °C of AP PPII in water. At this temperature, AP is fully in the PPII conformation. (b) 2,3,3,3-deuterated poly(alanine) PPII in water. This is a calculated spectrum where the contributions of nondeuterated residues were numerically subtracted. (c) AP PPII in D_2O. At this temperature, AP is fully in the PPII conformation. (d) 2,3,3,3-deuterated poly(alanine) PPII in D_2O. This is a calculated spectrum where the contributions of nondeuterated residues were numerically subtracted.

Results and Discussion

Assignment of the Amide III Region Bands (1230—1410 cm^{-1}) of AP in its PPII Conformation. Figure 1 shows the 204-nm excited UVRS[55] of the PPII conformation of AP in H_2O and D_2O, as well as the calculated spectrum of the PPII conformation of an isotopically substituted AP where 14 Ala were perdeuterated. We designate the intense 1245-cm^{-1} band of the PPII conformation of AP in water as the "classical" AmIII band, because it shows the largest dependence upon peptide bond conformational changes (vide infra).

This band, which disappears upon N-deuteration, also shows the large −0.15 cm^{-1}/°C frequency temperature dependence typical for the AmIII and AmII bands of non-α-helical and non-β-sheet peptides and simple amides such as *N*-methylacetamide (NMA, Figure 2). This temperature coeficient of −0.15 cm^{-1} is higher than the −0.1 cm^{-1} temperature reported earlier by Lednev et al.[2] for A_5—A_3. We measured the AP temperature coefficient from high *S*/*N* spectra at +49 °C and +65 °C.

For NMA, the AmII and III bands shift by −0.11 and −0.09 cm^{-1}/°C, while the AmI band shifts up by a much smaller amount. This temperature dependence derives from the decrease in hydrogen bonding by water as the temperature increases.[56,57] The mode frequencies decrease as the weakened water hydrogen bonding decreases the amide N—H bending and the C—N stretching force constants.[9,56,58]

This conclusion is evident from the temperature dependence of N-deuterated NMA (NMAD). The substitution of the much heavier N—D decouples N—D bending from C—N stretching,

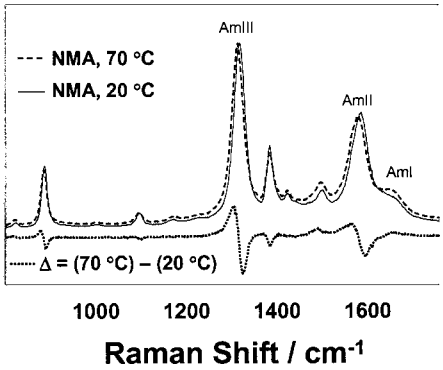

Figure 2. Temperature dependence of the 204-nm UVRS of *N*-methylacetamide and the 70 − 20 °C difference spectrum.

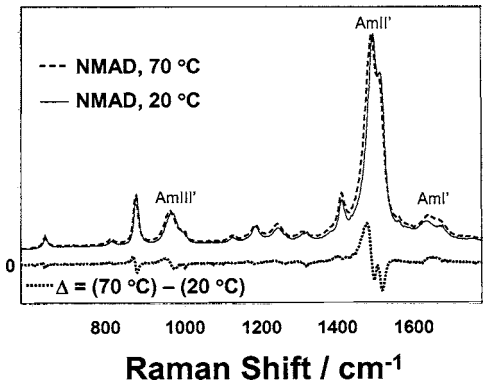

Figure 3. 204-nm excited UVRS temperature dependence of NMAD showing the large downshift of the 965-cm^{-1} AmIII′ band and the smaller downshift of the AmII′ doublet. The AmI′ band slightly upshifts and changes band shape.

and we have almost a pure C−N stretch which appears as a Fermi resonance doublet[59] at ∼1500 cm^{-1} (Figure 3).

We find that changes in water hydrogen bonding impact the N−D bend force constant more than the C−N stretch force constant; NMAD shows a smaller −0.07 cm^{-1}/°C temperature dependence of the mainly C−N stretching AmII′ band, compared to the −0.11 cm^{-1}/°C frequency decrease in the N−D bending-dominated NMAD AmIII′ band at 965 cm^{-1} (Figure 3). If an analogous pure N−H bending mode occurred at ∼1400 cm^{-1}, it would show a significantly larger temperature dependent frequency shift of ∼−0.16 cm^{-1}/°C.

This result indicates that the change in water hydrogen bonding impacts the N−H bending coordinate motions significantly more than the C−N stretching coordinates. The C_α−H bending bands show no temperature dependence, while the C═O stretching-dominated AmI bands of peptides and NMA show only a small positive frequency dependence on temperature. Small anhydrous peptide crystals show a negligible temperature dependence (data not shown).

Thus, a significant temperature dependence signals significant contributions of N−H bending and C−N stretching to a Raman band. From this, we conclude that the 1245-cm^{-1} PPII AP band in water contains a significant contribution of N−H ib and C−N stretching. Thus, the 1245-cm^{-1} PPII AP band can be clearly assigned to the classical AmIII vibration.

2,3,3,3-deuteration of the Ala side chains and C_α positions shifts the 1245-cm^{-1} PPII AP band to 1320 cm^{-1} (Figure 1). The 1320-cm^{-1} band shows a significant, but somewhat smaller, temperature dependence (−0.07 cm^{-1}/°C) than the 1245-cm^{-1} band. This band also disappears on N−H deuteration. Thus, this vibration contains significant fractions of N−H ib and C−N stretching. The main difference is that this vibration no longer

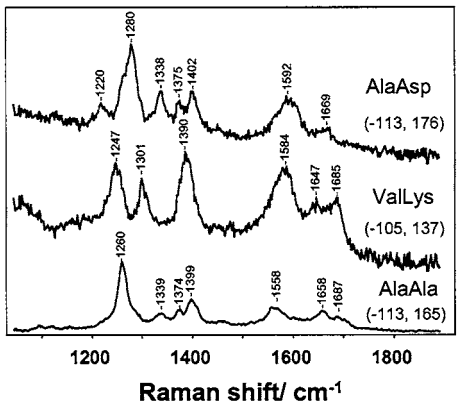

Figure 4. 229-nm excited UVRS of dipeptide crystal powders. Also shown are the Φ and Ψ dihedral angles obtained from the X-ray crystal structures.

contains C_α−H bending. This 81-cm^{-1} frequency shift on deuteration is heartwarmingly close to that expected from the relationship proposed by Asher et al.,[7,9] which correlates the AmIII band frequency to the extent of AmIII and C_α−H sb coupling (υ = 1265 cm^{-1} − 46.8 cm^{-1} sin(Ψ + 5.2°)).

The 1303-cm^{-1} and 1337-cm^{-1} bands of PPII AP in water disappear upon N−D deuteration, which suggests significant contributions from N−H bending. However, this is contradicted by the fact that the 1303- and 1337-cm^{-1} bands show only a small temperature dependence. The much weaker bands at 1284 and 1328 cm^{-1}, which occur in D_2O, could possibly be remnants of the 1303- and 1337-cm^{-1} bands if the new modes in D_2O lost contributions of C−N, C═O, C−C, and N−C motions that gave rise to their original resonance Raman enhancements.

A more likely explanation is that the existence of the 1303- and 1337-cm^{-1} normal modes of PPII AP depend sensitively on their N−H contributions. The removal of the N−H bending component could alter their vibrational mode compositions sufficiently that the resulting modes would shift outside the 1250−1400-cm^{-1} region.

Dipeptides such as AA, AD, and VK also show bands at these frequencies (1300 and 1340 cm^{-1}), which often appear overlapped either in solution on in crystal, as is evident from the resonance Raman spectra of crystals of dipeptides shown in Figure 4, along with their Φ and Ψ dihedral angles determined from their crystal structures. Ala-Asp and Ala-Ala, which have β-strand-like Ψ angles, show an ∼1338-cm^{-1} band, while the PPII-like Ψ = 137° of Val-Lys shows only a 1301-cm^{-1} band. We assume the 1301- and ∼1338-cm^{-1} bands have similar origins to those of PPII AP. From their small temperature dependence (Figure 5) and their large conformational dependence, we assign these bands to vibrations mainly involving C−C_α stretching mixed with C_α−H bending.

Our assignment appears to contradict that of Diem and coworkers,[48] who unequivocally assigned the 1336-cm^{-1} band in Ala-Ala to an unperturbed N−H deformation motion. The future will further illuminate the assignments of this complex spectral region.

Figure 6 shows the dependence of the 204-nm UVRS of increasingly long alanine peptides. Ala-Ala shows a much stronger 1337-cm^{-1} band than occurs in the larger peptides; the decreased intensity observed for the 1337-cm^{-1} band in the Ala-Ala crystals may be due to its preresonance excitation at 229 nm, to the red of the amide $\pi \rightarrow \pi^*$ transition.

The relative intensity of the 1337-cm^{-1} band smoothly decreases as the peptide length increases to A_6 (Figure 6). The various difference spectra between these peptides shown in

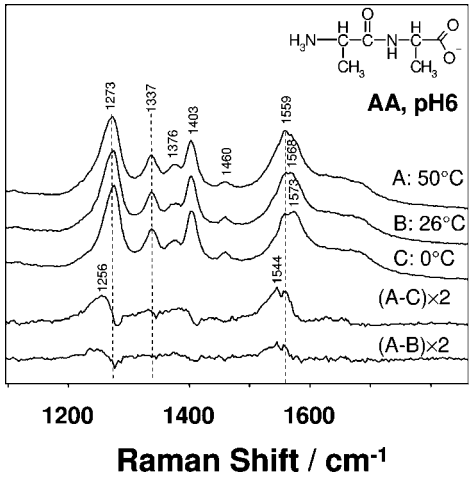

Figure 5. Temperature dependence of the 229-nm UVRS spectra of AA in water. Power, 5 mW; sample concentration, 5 mg/mL; spectral resolution, 8 cm^{-1}.

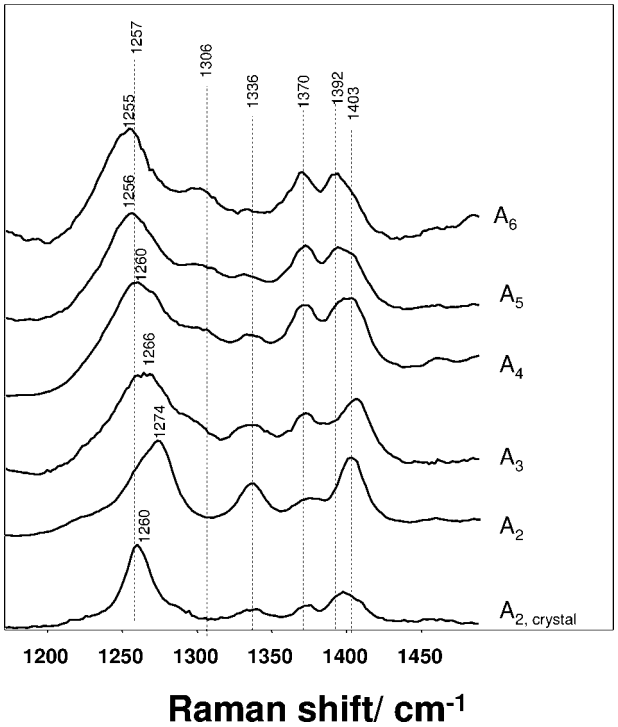

Figure 6. 204-nm UVRS spectra of different poly(Ala) in water and the 229-nm UVRS of A2 crystal powder

Figure 7 display no feature close to 1337 cm^{-1} for peptides larger than Ala_3. Thus, the existence of a small peak in AP at this frequency at elevated temperatures is quite surprising. This 1337-cm^{-1} peak clearly derives from AP, which is predominantly PPII at this temperature. It does not derive from small peptide fragments, because HPLC−MS analysis of AP samples clearly demonstrates the absence of significant hydrolysis or photolysis to smaller fragments. Temperature difference spectra between 50 and 80 °C show a small intensity increase and broadening of this band.

This band must signal a minority population of some conformation of AP. It is impossible at this point to determine the nature of this conformation solely from the spectra, because the 1337-cm^{-1} band appears in both β-strand and α-helix-like conformations. We would need to resolve whether the other bands which are signatory of non-PPII conformations are also present in the underlying spectra. It is most likely, however,

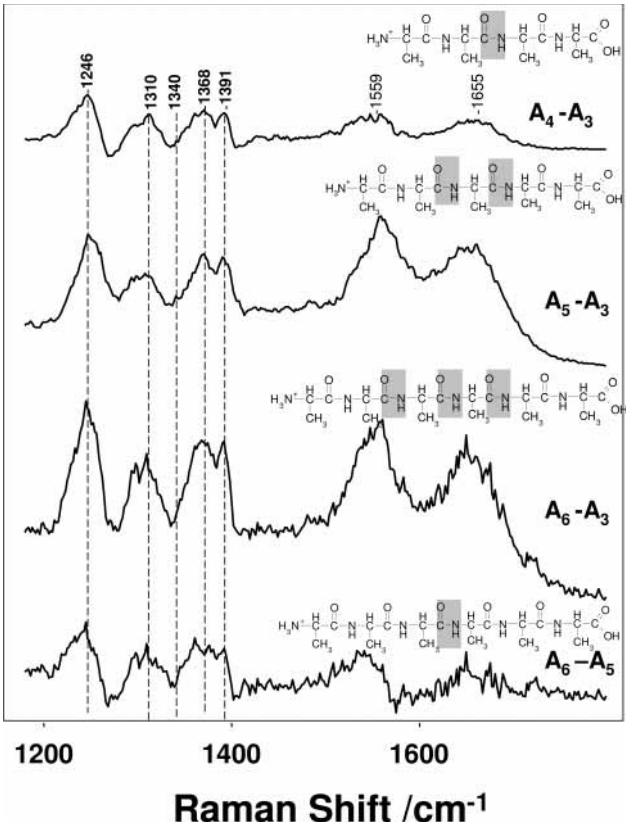

Figure 7. 204-nm UVRS difference spectra between different poly-(Ala) in water.

that this small band derives from a small β-strand contribution, in view of the known occurrence of minor β-strand contributions to the mainly PPII conformation of the alanine-rich XAO peptide.[60]

Assignment of the Amide I Region Bands of AP in its PPII Conformation. The N−D PPII state of AP and AdP in D_2O both show two bands in the AmI′ region at ∼1614 and ∼1660 cm^{-1} (Figure 1). The 1660-cm^{-1} band shows the expected temperature dependence of the AmI band, in which it slightly upshifts in frequency as the temperature increases. In contrast, the 1614-cm^{-1} band shows a negligible temperature dependence. As shown below, the 1614-cm^{-1} band derives from an R side chain vibration, while the ∼1660-cm^{-1} band is the AmI′ band.

Assignment of the Amide III Region Bands of AP in the α-Helical Conformation. Figure 8 shows the calculated 204-nm UVRS of α-helical AP, and of its perdeuterated derivative in both water and D_2O. These α-helical spectra were calculated by removing contributions from PPII conformations and, in the cases of the perdeuterated derivatives, from protonated amino acids in the chain. The details are described in the figure caption.

The UVRS of α-helical AP displays a triplet of bands at 1261 ($AmIII_3$), 1303 ($AmIII_2$), and 1337 cm^{-1} ($AmIII_1$) in the amide III region. We should caution that there is no implication in this labeling scheme that the $AmIII_i$ bands of the α-helix correspond to the same labeled bands of the PPII conformation.

The temperature dependence of the entire α-helix spectrum is negligibly small below 10 °C (Figure 9), as originally noted by Lednev et al.[2,3,61−63] However, at temperatures above 20 °C, the spectrum shows a surprising downshift for the $AmIII_3$ band, which is accompanied by an AmI band shape change and the appearance of an additional, AmI_1 band (Figure 10). The decreased *S*/*N* of the higher temperature α-helix spectra displayed in Figure 9 is due to the decreased α-helical fractions

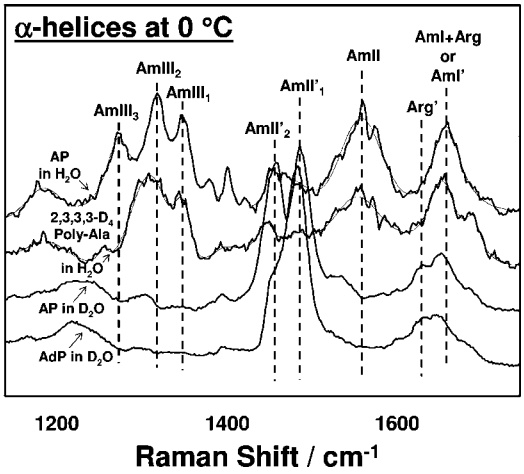

Figure 8. Calculated 204-nm UVRS α-helical spectra of AP and its isotopically substituted derivatives at 0 °C. (a) α-helical AP in water. This spectrum was obtained by subtracting the 0 °C calculated AP PPII spectrum from the measured 0 °C AP spectrum (∼45% PPII). (b) 2,3,3,3-deuterated poly-L-(alanine) α-helix in water where the contribution from the protonated amides was numerically removed. This spectrum was obtained by subtracting the calculated 0 °C AdP PPII spectrum from the measured 0 °C AdP spectrum, followed by subtraction of the appropriate amount of 0 °C AP α-helix spectrum. (c) α-helical AP in D_2O. This spectrum was obtained by subtracting the 0 °C AP PPII spectrum from the experimental 0 °C AP spectrum (∼45% PPII). (d) α-helical AdP in D_2O. This spectrum was obtained by subtracting the 0 °C AdP PPII spectrum from the experimental 0 °C AdP spectrum (∼45% PPII). Note that AdP sequence contains fourteen 2,3,3,3-deuterated Ala, 4 nondeuterated Ala, and 3 nondeuterated Arg.

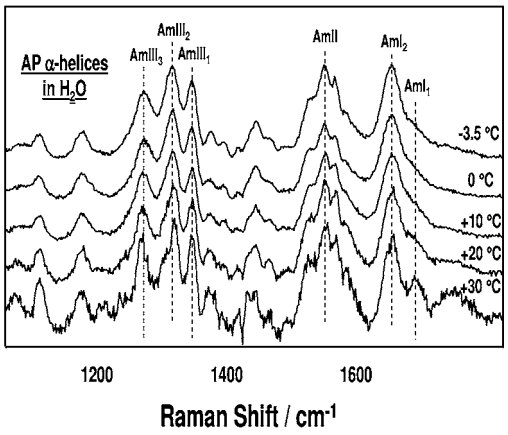

Figure 9. Calculated temperature dependence of 204-nm UVRS of α-helical AP in water. The spectra were calculated by subtracting the appropriate amount of PPII AP spectrum from the measured spectrum at the corresponding temperature. The low *S*/*N* of the AmII band results from the incomplete subtraction of the Raman band of O_2.

of AP at +20 and +30 °C, compared to those[2,3,61−63] at −3.5, 0, and +10 °C.

We suggest that these spectral changes result from an α-helix hydration change at higher temperatures. The poly(Ala) α-helix should be well hydrated by water.[56,58,64−68] The temperature increase should decrease the extent of hydration of a fraction of the α-helical peptide bonds because of the decrease in the water−peptide hydrogen bonding strength.[58,68] This then shifts those bands with significant N−H b and C−N s to lower frequency and shifts the AmI band to higher frequency. The new AmI_1 band is shifted to 1682 cm^{-1}, which may be a signature of a nonhydrated helix.

Obviously, our spectral changes are discontinuous, and a transition appears around 20 °C, yielding a partially dehydrated

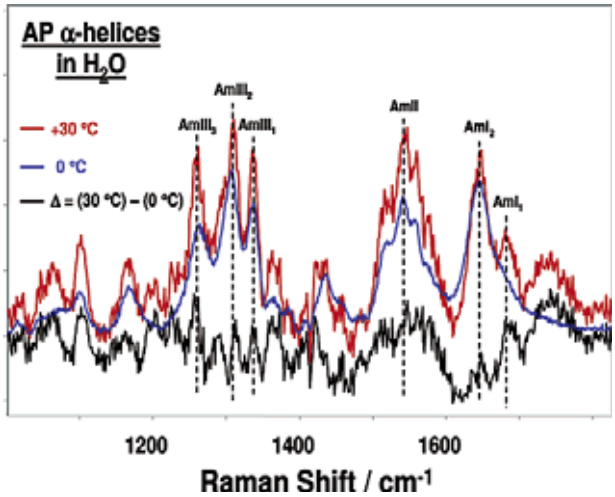

Figure 10. UVRS of α-helical AP at 0 and 30 °C and their difference spectrum showing the downshift of $AmIII_3$ and the appearance of a higher frequency AmI_1 band.

helix. Possibly, these dehydrated helix segments are an intermediate in the α-helix to a PPII conformational transition. The dehydrated helical segments may have an increased propensity to evolve into the PPII form, because a temperature increase raises the free energy of partially dehydrated α-helical segments above that of the PPII conformation.

Whatever the case, we conclude that the $AmIII_3$ band contains a large amount of N−H bending. Therefore, we label the 1261-cm^{-1} band as the "classical AmIII band".

This triplet of bands disappears upon N-deuteration (Figure 8), leaving only a very weak ∼1293-cm^{-1} band. The spectral intensities can be referenced to a constant AmI band intensity, because the AmI cross sections change little with temperature, conformation, or isotopic substitution.

The AmII′ doublet of AP in D_2O is replaced by a singlet in the perdeuterated derivative AdP in D_2O because of a loss of the Fermi resonance between C−N s and CH_3 bending.[59] However, the AdP spectrum still shows some remnant of the doublet because of the contribution of the AmII′ doublet from the four non-perdeuterated Ala residues.

The largest change that occurs upon the perdeuteration of α-helical AP is the disappearance of the $AmIII_3$ band, which leaves behind a doublet spectral contour (Figure 8). We attempted to determine whether the $AmIII_3$ band disappeared or whether it shifted underneath the doublet. Unfortunately, the Figure 11 deconvolution attempt does not by itself definitively resolve whether two or three bands underlie the broad doublet contour of perdeuterated α-helical AP. The contour can be fit by two bands if the lower frequency band is allowed to have a >50-cm^{-1} bandwidth. However, a more likely conclusion is that a triplet of ∼30-cm^{-1} bandwidth bands at 1284, 1308, and 1335 cm^{-1} underlies this contour; the 50-cm^{-1} bandwidth appears unphysically large.

Some shift of the $AmIII_3$ band to higher frequency upon C_α deuteration is consistent with the expectation[7] that the AmIII band frequency depends on coupling between N−H and C_α−H motions of two essentially degenerate vibrations. However, because the C_α−H and N−H bonds are trans in the α-helix conformation, we expect only a small shift. It should be noted, however, that the $AmIII_3$ band might also contain contributions of other components of C_α−H motion, whose removal might cause a frequency upshift, resulting in the overlap of the original $AmIII_1$ and $AmIII_2$ bands with the $AmIII_3$ band blue-shifted to ∼1326 cm^{-1}.

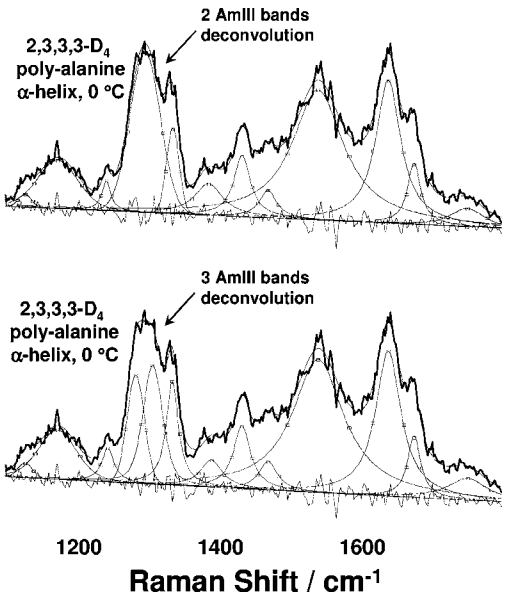

Figure 11. Attempts to deconvolute the Ala perdeuterated α-helix AP AmIII region into a doublet and triplet of underlying bands.

In contrast, we conclude that the $AmIII_3$ band disappears if we consider the resonance Raman intensities and expect that the integrated Raman cross-section would be conserved if the $AmIII_3$ band shifts into the doublet contour. We utilized the measured intensity ratio of the AmIII band envelope relative to the AmI band(s) to determine whether the doublet envelope contains the $AmIII_3$ band. We assume that the resonance Raman enhancement of these Raman bands derive from their C—N s, C═O s, C_α—CO s, and N—C s motions.[59] Our analysis requires that isotopic substitution does not perturb the electronic transitions and that the loss of C_α—H bending does not change the Raman intensities. If the $AmIII_3$ band shifts underneath the doublet contour, the integrated intensity within the contour, relative to that of the AmI band (whose intensity remains relatively constant) would remain identical to that of natural abundance α-helical AP. In contrast, the ratio decreases almost 2-fold in the perdeuterated derivative, suggesting that the band disappears. Thus, we are unable to come to a definitive conclusion of what happens to the $AmIII_3$ band in the deuterated derivative.

Thus, we assign the 1261-cm^{-1} band to the classical AmIII structure of an α-helix conformation, which as pointed out by Lee and Krimm, involve C—N s and N—H b. It may also contain some C_α—C s.

We assign the 1306-cm^{-1} band of natural abundance α-helical AP to a vibration which involves mainly C—C and N—C stretching, because this band shows little temperature dependence and may be slightly affected by hydration (Figure 9). This band is not conformationally sensitive, because it shows up in both the α-helix (∼1306 cm^{-1}) and the PPII (∼1303 cm^{-1}) conformations. The assignments of the other bands are indicated above.

We should note the recent results of Overman et al.,[27] who examined the impact of Ala C_α—D substitution on normal Raman α-helical virus coat proteins. Upon replacement of C_α—H, they observe that a 1345-cm^{-1} band shifts to 1296 cm^{-1}. This behavior is almost exactly the opposite of what we observe. Barron et al.[69−71] also have observed a hydrated α-helix band at ∼1345 cm^{-1} with visible excitation ROA. We see no hydration dependence for our 1337-cm^{-1} band. Thus, we conclude that their hydrated ∼1345-cm^{-1} α-helix band is not enhanced upon 204-nm resonance excitation.

Assignment of Other Amide Bands of AP in the α-Helical Conformation. The intensity of the 1380-cm^{-1} band of α-helical AP in D_2O decreases significantly in AdP in D_2O (Figures 1 and 8). This observation is completely consistent with the assignment of this band to mainly the CH_3 sb mode of Ala side chain by Lee and Krimm,[49] because AdP contains only 4 non-perdeuterated Ala residues, while AP contains 18 non-perdeuterated Ala.

The 1614-cm^{-1} band, which shows up in the UVRS spectra of both α-helical and PPII states of AP and AdP in D_2O (Figures 1 and 8) cannot be assigned to the AmI′ band, because it is not conformationally sensitive, and it does not show the temperature dependence typical of the AmI bands. We assign this band to an arginine side-chain C—N s mode on the basis of Chi et al.'s[5] UVRS of Arg. The observed 1630-cm^{-1} Arg band in water downshifts in D_2O.[54]

Tables 1 and 2 summarize the spectroscopic information used to assign the amide III region of the PPII and α-helical conformations of AP.

Comparison between UVRS of α-Helical and PPII Conformations of AP and AdP. Figure 12 compares the UVRS of

TABLE 1: Assignments, Isotopic and Temperature Dependencies of Amide III Region UV Raman Bands of the PPII Conformation of AP

UVR band assignment	conformational dependence	NH/ND substitution	C_α—D substitution	*T* dependence	included atomic motion	excluded atomic motion
1245 cm^{-1} classical amide III	most sensitive to conformation	disappears with AmIII′ band appearing at ∼950−1000 cm^{-1}	shifts to 1326 cm^{-1} (NH b and CN s)	large	N—H b coupled to C_α—H b and CN stretch	none
1303 cm^{-1}	no?	disappears	transforms to shoulder at 1278 cm^{-1}?	moderate	stretches of heavy atoms, C_α—C s, N—C s, C—N s + some C_α—H b	N—H b
1337 cm^{-1}	originates from extended β-strand-like conformation?	disappears	hidden under the broad ∼1326 cm^{-1} envelope?	small	C_α—C s and N—C s	N—H b C—N s
1370 cm^{-1}	most sensitive to conformation	disappears	disappears	none	C_α—H b, C_α—C s, CH_3 umbrella. maybe small amount C—N s	N—H b
1394 cm^{-1}	most sensitive to conformation	disappears	disappears	none	C_α—H b, C_α—C s maybe small amount of C—N s	N—H b

TABLE 2: Assignments and Isotopic and Temperature Dependence of Amide III Region UV−Raman Bands of the α-Helical Conformation of AP

band assignment	conformational dependence	NH/ND substitution	C_α−D and CD_3 substitution	*T* dependence	hydration dependence	included atomic motions	excluded atomic motions
1261 cm^{-1} classical amide III	most sensitive to conformation?	disappears with AmIII′ band appearing at ∼950−1000 cm^{-1}	???	strong	most sensitive to hydration	N−H b, C−N s , and maybe C_α−C	none
1306 cm^{-1}	not sensitive	disappears	either shifts to ∼1284 cm^{-1} or remains at ∼1308 cm^{-1}	small	only slightly influenced by hydration	C_α−C s, N−C s, and small amount of C−N s	N−H b, and maybe C_α−H b
1337 cm^{-1}	not sensitive	disappears	remains at the same position?	no	no	C_α-C s, N−C s, and maybe small amount of C−N s	N−H b, C_α−H b

the α-helix and PPII conformations of AP. As found earlier by Chi et al.,[5] the intense PPII ∼1245-cm^{-1} $AmIII_3$ band and the intense ∼1400-cm^{-1} C_α−H sb band (called incorrectly random coil[2,3,61−63]) dramatically decrease in intensity in the α-helix conformation and are replaced by a broad envelope of bands centered at ∼1300 cm^{-1}. The ∼1400-cm^{-1} C_α−H sb band contour in PPII disappears completely and is replaced by a weak band at ∼1390 cm^{-1} due to the methyl umbrella mode. The intensity of the PPII AmII band decreases by more than 2-fold, while its frequency downshifts by ∼12 cm^{-1} in the α-helix. The peak height intensity of the AmI band remains essentially constant, while its frequency downshifts by ∼13 cm^{-1}.

The decrease in intensity results from a decrease in the oscillator strength of the amide $\pi \rightarrow \pi^*$ transition due to excitonic interactions in the α-helical conformation.[40,72−76] This is clearly evident in the Figure 13 comparison between the α-helix and PPII UVRS of AP and AdP in D_2O. Resonance Raman enhancement is dominated by the AmII′ band which is mainly C−N s.[59] The intensity of the AmI′ band stays constant while the integrated intensity of the AmII′ band of the α-helix conformation decreases by more than 2-fold for AP and AdP. In contrast, the Figure 14 AmII′ comparison between AP and AdP conformations show that the enhancement remains relatively constant even though AdP residues are deuterated. The small AmII′ enhancement decrease in PPII AP is made up by small enhancement increases for the AmIII′ band as well as other small bands. For the α-helix, essentially identically enhanced AmII′ bands occur.

The Figure 12 UVRS display the significant spectral changes which occur between the PPII and α-helix conformations of natural-abundance AP in H_2O. The maximum changes occur in the Amide III spectral region. It is not possible to assign bands of the PPII and α-helix conformations to similar vibrations, but the $AmIII_3$ vibrations of both conformations seem to have both N−H b and C−N s contributions. For example, the ∼1245-cm^{-1} $AmIII_3$ band of PPII has significant N−H bending and C−N s as evident from the −0.15 cm^{-1}/°C temperature coefficient. Similarly, the α-helix $AmIII_3$ band shows a −0.15 cm^{-1}/°C temperature coefficient between 10 and 30 °C (while showing no temperature dependence below 10 °C). This agrees well with Lee and Krimm,[50] who calculate a band at 1263 cm^{-1} which is dominated by N−H bending, which also contains a large component of C−N s which gives rise to enhancement.

The bands labeled $AmIII_1$ and $AmIII_2$ of PPII and α-helical conformations significantly differ. Perhaps this point is most succinctly shown by the differences between the calculated

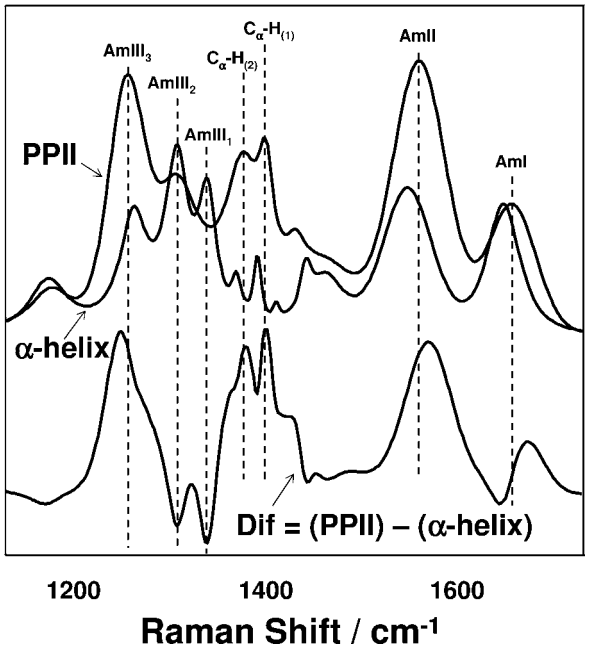

Figure 12. Comparison of the 204-nm calculated UVRS of the α-helix and PPII conformations of AP at 0 °C and their difference spectrum.

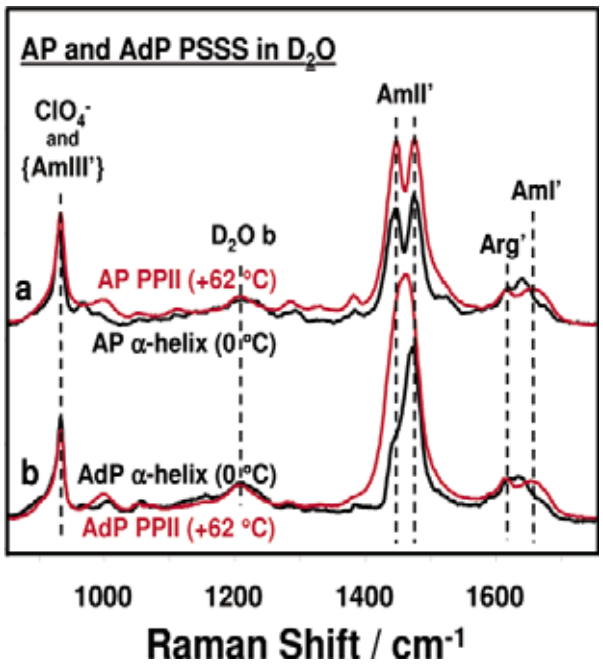

Figure 13. Comparison between measured PPII and calculated α-helix AP and AdP in D_2O UVRS.

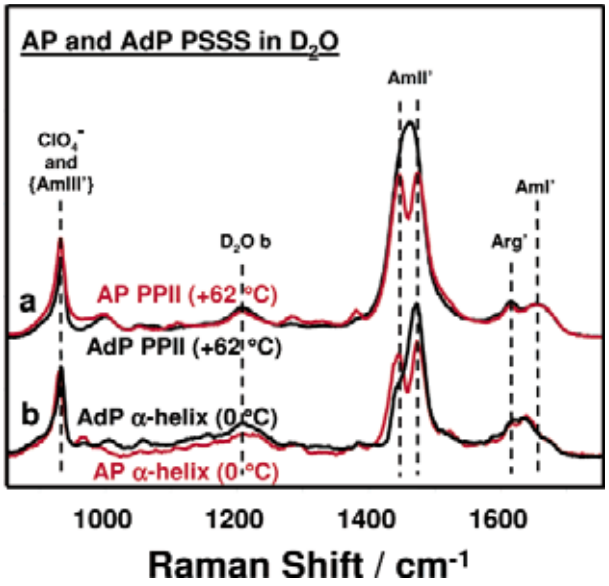

Figure 14. Comparison of measured PPII and calculated α-helix AP and AdP in D_2O UVRS.

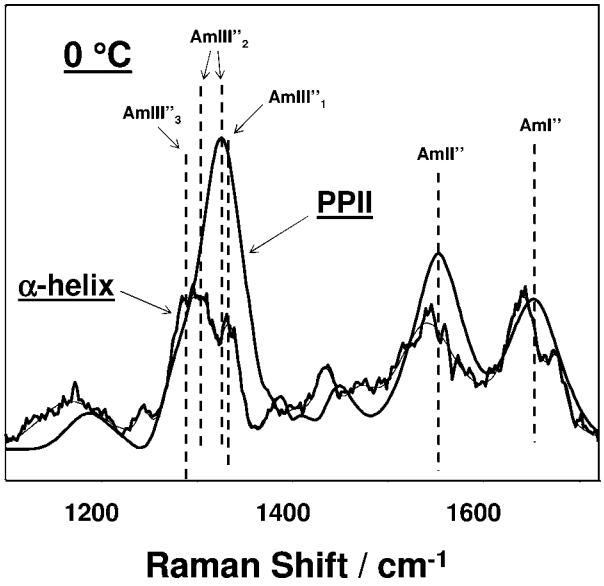

Figure 15. Comparison of calculated UVRS of PPII and α-helix of fully 2,3,3,3-D_4 deuterated A_{21}.

UVRS of PPII and α-helix conformations of fully perdeuterated AP (Figure 15). Even though deuteration has removed coupling with the $C_\alpha-H$ b, significant differences occur in the Amide III region, in addition to the hypochromic α-helix spectral intensity decrease.

This investigation of the melting of AP from the α-helix to PPII conformations indicates that the melting can be quantitated by the characteristic difference spectra displayed in Figure 12. Obviously, these difference spectra will change at different temperatures due to the temperature dependence of the basis spectra.

Although we expect that the other α-helix peptide conformations will show qualitatively similar spectra, we expect to also see significant differences because of the fact that the side chains differ, the environments differ, and the α-helix exposure to solvent and its resulting hydration may differ.[56,58,68] This is clearly evident in the Figure 16 UVRS spectral temperature dependence of the mainly α-helical apoMb. The contributions from the unordered states of apoMb were numerically removed by subtracting the acid-denatured apoMb spectra from the neutral-pH apoMb spectra. The resulting overlapped AmIII triplet contour α-helix apoMb spectra shows little temperature dependence even up to 56 °C.

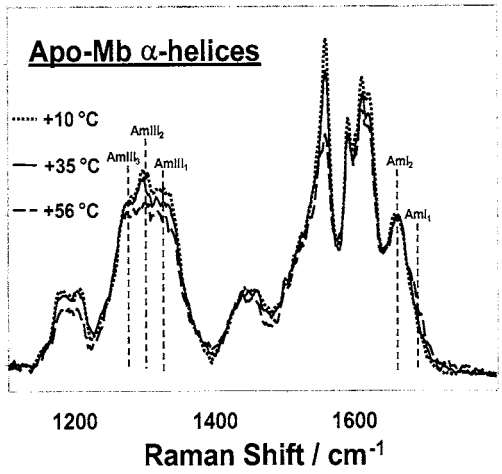

Figure 16. Temperature dependence of the UVRS of apoMb α-helices. Non-α-helical spectral contributions were removed by subtracting pH = 1.86 unordered apoMb spectra.

The spectral temperature changes observed are significantly smaller than in α-helical AP (at $T > +10$ °C). The largest change is the blue-shift of the AmI band high-frequency edge which shows up at the highest temperatures. Obviously, the apoMb α-helices are much more stable and show much less hydration change than are observed for AP, which is monomeric and fully water exposed.

Careful UV Raman studies of proteins may be able to monitor subtle effects such as helix hydration changes, in addition to being able to monitor the larger conformational changes.

Conclusions

We have reexamined in detail the assignment of the amide III region of the PPII and α-helix conformations of peptides and proteins using UV Raman spectra of a mainly poly(Ala) peptide. Many of our assignments agree with previous studies, while others challenge the conventional understanding. The conformational dependence of the UVRS spectra make this methodology a sensitive probe of protein and peptide secondary structure. We appear to see spectral signatures of α-helix hydration changes with temperature.

Acknowledgment. The authors would like to thank Sergei Bykov, Dr. Noemi Mirkin, and Dr. Nataliya Myshakina for helpful discussions, as well as NIH grant 8 RO1 EB002053021 for financial support.

References and Notes

(1) Asher, S. A. *Handbook of Vibrational Spectroscopy*; John Wiley & Sons: New York, 2001; Vol. 1, p 557.
(2) Lednev, I. K.; Karnoup, A. S.; Sparrow, M. C.; Asher, S. A. *J. Am. Chem. Soc.* **1999**, *121*, 8074.
(3) Lednev, I. K.; Karnoup, A. S.; Sparrow, M. C.; Asher, S. A. *J. Am. Chem. Soc.* **2001**, *123*, 2388.
(4) Gruebele, M. *Annu. Rev. Phys. Chem.* **1999**, *50*, 485.
(5) Chi, Z.; Chen, X. G.; Holtz, J. S. W.; Asher, S. A. *Biochemistry* **1998**, *37*, 2854.
(6) Schweitzer-Stenner, R. *J. Raman Spectrosc.* **2001**, *32*, 711.
(7) Asher, S. A.; Ianoul, A.; Mix, G.; Boyden, M. N.; Karnoup, A.; Diem, M.; Schweitzer-Stenner, R. *J. Am. Chem. Soc.* **2001**, *123*, 11775.
(8) Ianoul, A.; Boyden, M. N.; Asher, S. A. *J. Am. Chem. Soc.* **2001**, *123*, 7433.
(9) Asher, S. A.; Mikhonin, A. V.; Bykov, S. V. *J. Am. Chem. Soc.* **2004**, *126*, 8433.
(10) Badger, R. M. *Annu. Rev. Phys. Chem.* **1955**, *6*, 217.

(11) Chen, M. C.; Lord, R. C. *J. Am. Chem. Soc.* **1974**, *96*, 4750.
(12) Chen, M. C.; Lord, R. C.; Mendelsohn, R. *Biochim. Biophys. Acta* **1973**, *328*, 252.
(13) Hamm, P.; Lim, M.; DeGrado, W. F.; Hochstrasser, R. M. *Proc. Natl. Acad. Sci. U.S.A.* **1999**, *96*, 2036.
(14) Chen, Z.; Shen, Y. R.; Somorjai, G. A. *Annu. Rev. Phys. Chem.* **2002**, *53*, 437.
(15) Woutersen, S.; Hamm, P. *J. Chem. Phys.* **2001**, *114*, 2727.
(16) Speare, J. O.; Rush, T. S., III *Biopolymers* **2003**, *72*, 193.
(17) Venyaminov, S.; Prendergast, F. G. *Anal. Biochem.* **1997**, *248*, 234.
(18) Torrecillas, A.; Corbalan-Garcia, S.; Gomez-Fernandez, J. C. *Biochemistry* **2004**, *43*, 2332.
(19) Wu, Y.; Murayama, K.; Ozaki, Y. *J. Phys. Chem. B* **2001**, *105*, 6251.
(20) Prestrelski, S. J.; Byler, D. M.; Thompson, M. P. *Intl. J. Pept. Protoien Res.* **1991**, *37*, 508.
(21) Keiderling, T. A. *Curr. Opin. Chem. Biol.* **2002**, *6*, 682.
(22) Keiderling, T. A. *Circular Dichroism*, 2nd ed.; 2000, p 621.
(23) Tanaka, T.; Inoue, K.; Kodama, T.; Kyogoku, Y.; Hayakawa, T.; Sugeta, H. *Biopolymers* **2001**, *62*, 228.
(24) Wang, F.; Polavarapu, P. L. *J. Phys. Chem. B* **2001**, *105*, 7857.
(25) Baello, B. I.; Pancoska, P.; Keiderling, T. A. *Anal. Biochem.* **1997**, *250*, 212.
(26) Kocak, A.; Luque, R.; Diem, M. *Biopolymers* **1998**, *46*, 455.
(27) Overman, S. A.; Thomas, G. J., Jr. *Biochemistry* **1998**, *37*, 5654.
(28) Mizuno, A.; Fujii, N.; Akaboshi, M.; Momose, Y.; Shimo-oka, T. *Jpn. J. Ophthalmol.* **2000**, *44*, 354.
(29) Colaianni, S. E. M.; Aubard, J.; Hansen, S. H.; Nielsen, O. F. *Vib. Spectrosc.* **1995**, *9*, 111.
(30) Copeland, R. A.; Spiro, T. G. *Biochemistry* **1987**, *26*, 2134.
(31) Sane, S. U.; Cramer, S. M.; Przybycien, T. M. *Anal. Biochem.* **1999**, *269*, 255.
(32) Overman, S. A.; Thomas, G. J., Jr. *Biochemistry* **1995**, *34*, 5440.
(33) Overman, S. A.; Thomas, G. J., Jr. *Biochemistry* **1999**, *38*, 4018.
(34) Dudik, J. M.; Johnson, C. R.; Asher, S. A. *J. Phys. Chem.* **1985**, *89*, 3805.
(35) Wilson, G.; Hecht, L.; Barron, L. D. *Biochemistry* **1996**, *35*, 12518.
(36) McColl, I. H.; Blanch, E. W.; Gill, A. C.; Rhie, A. G. O.; Ritchie, M. A.; Hecht, L.; Nielsen, K.; Barron, L. D. *J. Am. Chem. Soc.* **2003**, *125*, 10019.
(37) McColl, I. H.; Blanch, E. W.; Hecht, L.; Kallenbach, N. R.; Barron, L. D. *J. Am. Chem. Soc.* **2004**, *126*, 5076.
(38) Nafie, L. A.; Yu, G.-S.; Freedman, T. B. *Vib. Spectrosc.* **1995**, *8*, 231.
(39) Yu, G.-S.; Freedman, T. B.; Nafie, L. A.; Deng, Z.; Polavarapu, P. L. *J. Phys. Chem.* **1995**, *99*, 835.
(40) Song, S.; Asher, S. A. *J. Am. Chem. Soc.* **1989**, *111*, 4295.
(41) Wang, Y.; Purrello, R.; Georgiou, S.; Spiro, T. G. *J. Am. Chem. Soc.* **1991**, *113*, 6368.
(42) Wang, Y.; Purrello, R.; Spiro, T. G. *J. Am. Chem. Soc.* **1989**, *111*, 8274.
(43) Jordan, T.; Spiro, T. G. *J. Raman Spectrosc.* **1994**, *25*, 537.
(44) Jordan, T.; Mukerji, I.; Wang, Y.; Spiro, T. G. *J. Mol. Struct.* **1996**, *379*, 51.
(45) Mirkin, N. G.; Krimm, S. *J. Phys. Chem. A* **2002**, *106*, 3391.
(46) Oboodi, M. R.; Alva, C.; Diem, M. *J. Phys. Chem.* **1984**, *88*, 501.
(47) Diem, M.; Polavarapu, P. L.; Oboodi, M.; Nafie, L. A. *J. Am. Chem. Soc.* **1982**, *104*, 3329.
(48) Diem, M.; Lee, O.; Roberts, G. M. *J. Phys. Chem.* **1992**, *96*, 548.
(49) Lee, S.-H.; Krimm, S. *Biopolymers* **1998**, *46*, 283.
(50) Lee, S.-H.; Krimm, S. *Chem. Phys.* **1998**, *230*, 277.
(51) Lee, S.-H.; Krimm, S. *J. Raman Spectrosc.* **1998**, *29*, 73.
(52) Overman, S. A.; Thomas, G. J., Jr. *J. Raman Spectrosc.* **1998**, *29*, 23.
(53) Mix, G.; Schweitzer-Stenner, R.; Asher, S. A. *J. Am. Chem. Soc.* **2000**, *122*, 9028.
(54) Mikhonin, A. V.; Asher, S. A. Submitted to *J. Phys. Chem. B*, 2004.
(55) Note: We apologize for reversing the labeling scheme pioneered by Diem et al. (ref 48), but find it more logically consistent with the normal vibrational numbering scheme which numerates bands in the order of highest to lowest frequencies.
(56) Manas, E. S.; Getahun, Z.; Wright, W. W.; DeGrado, W. F.; Vanderkooi, J. M. *J. Am. Chem. Soc.* **2000**, *122*, 9883.
(57) Wernet, P.; Nordlund, D.; Bergmann; Carvalleri, M.; Odelius, M.; Ogasawara, H.; Naslund, L. A.; Hirsch, T. K.; Ojamae, L.; Glatzel, P.; Pettersson, L. G. M.; Nilsson, A. *Science* **2004**, *304*, 995.
(58) Walsh, S. T. R.; Cheng, R. P.; Wright, W. W.; Alonzo, D. O. V.; Daggett, V.; Vanderkooi, J. M.; DeGrado, W. F. *Protein Sci.* **2003**, *12*, 520.
(59) Chen, X. G.; Asher, S. A.; Schweitzer-Stenner, R.; Mirkin, N. G.; Krimm, S. *J. Am. Chem. Soc.* **1995**, *117*, 2884.
(60) Shi, Z.; Olson, C. A.; Rose, G. D.; Baldwin, R. L.; Kallenbach, N. R. *Proc. Natl. Acad. Sci. U.S.A.* **2002**, *99*, 9190.
(61) Lednev, I. K.; Karnoup, A. S.; Sparrow, M. C.; Asher, S. A. In *Spectroscopy of Biological Molecules: New Directions*; Eighth European Conference on the Spectroscopy of Biological Molecules, Enschede, The Netherlands, Aug. 29−Sept. 2, 1999; p 11.
(62) Lednev, I. K.; Karnoup, A. S.; Sparrow, M. C.; Asher, S. A. *J. Am. Chem. Soc.* **1999**, *121*, 4076.
(63) Lednev, I. K.; Karnoup, A. S.; Sparrow, M. C.; Asher, S. A. In *Abstracts of Papers,* 219th National Meeting of the American Chemical Society, San Francisco, CA, March 26−30, 2000; American Chemical Society: Washington, DC, 2000; PHYS.
(64) Ghosh, T.; Garde, S.; Garcia, A. E. *Biophys. J.* **2003**, *85*, 3187.
(65) Demmel, F.; Doster, W.; Petry, W.; Schulte, A. *Eur. Biophys. J.* **1997**, *26*, 327.
(66) Gerstein, M.; Lynden-Bell, R. M. *J. Phys. Chem.* **1993**, *97*, 2991.
(67) Gerstein, M.; Lynden-Bell, R. M. *J. Phys. Chem.* **1993**, *97*, 2982.
(68) Garcia, A. E. *Polymer* **2004**, *45*, 669.
(69) Blanch, E. W.; Bell, A. F.; Hecht, L.; Day, L. A.; Barron, L. D. *J. Mol. Biol.* **1999**, *290*, 1.
(70) Blanch, E. W.; Kasarda, D. D.; Hecht, L.; Nielsen, K.; Barron, L. D. *Biochemistry* **2003**, *42*, 5665.
(71) Blanch, E. W.; Robinson, D. J.; Hecht, L.; Syme, C. D.; Nielsen, K.; Barron, L. D. *J. Gen. Virol.* **2002**, *83*, 241.
(72) Robin, M. B. *Higher Excited States of Polyatomic Molecules*; Academic Press: New York, 1975; Vol. II.
(73) Schellman, J. A.; Becktel, W. J. *Biopolymers* **1983**, *22*, 171.
(74) Momii, R. K.; Urry, D. W. *Macromolecules* **1968**, *1*, 372.
(75) Onari, S. *Jpn. J. Appl. Phys.* **1970**, *9*, 227.
(76) Moffit, W. *Proc. Natl. Acad. Sci. U.S.A.* **1956**, *42*, 736.